The 33rd Annual Intelligent Ground Vehicle Competition

Hosei University
Autonomous Robotics Laboratory Team

Orange2026

Koki Shozawa koki.shozawa.3i@stu.hosei.ac.jp
Hiroki Tanaka hiroki.tanaka.3j@stu.hosei.ac.jp
Gondo Hiroki hiroki.gondo.8u@stu.hosei.ac.jp
Kentaro Hatori kentaro.hatori.3h@stu.hosei.ac.jp
Hinata Kasai hinata.kasai.8i@stu.hosei.ac.jp

Faculty Advisor Statement

I hereby certify that the engineering design for the Orange2026 Design Challenge (AutoNav and Self-Drive challenges) was completed by the current student team and is of a standard equivalent to work that would merit credit in a senior design course.

Signed Kazuyuki Kobayashi

Prof. Kazuyuki Kobayashi

Date
May 12,2026

Faculty of Science and Engineering, Hosei University
3-7-2 Kajinocho Koganei, Tokyo 184-8584, Japan
E-mail: ikko@hosei.ac.jp

3 System and Subsystem Requirements

3.1 System Engineering Process

In last year's Agile development process, we encountered structural challenges in maintaining flexibility. When issues arose during implementation, backtracking to the strategic planning phase for necessary adjustments proved difficult, making rapid corrections to the mobile robot's behavior time-consuming.

To address these challenges, we adopted the Observe, Orient, Decide, and Act (OODA) loop for the present project. This framework enables a continuous cycle of observation, decision-making, and execution, allowing for a swift response to changes in the desired behavior of the mobile robot. Figure 1 illustrates the concept of the OODA loop.

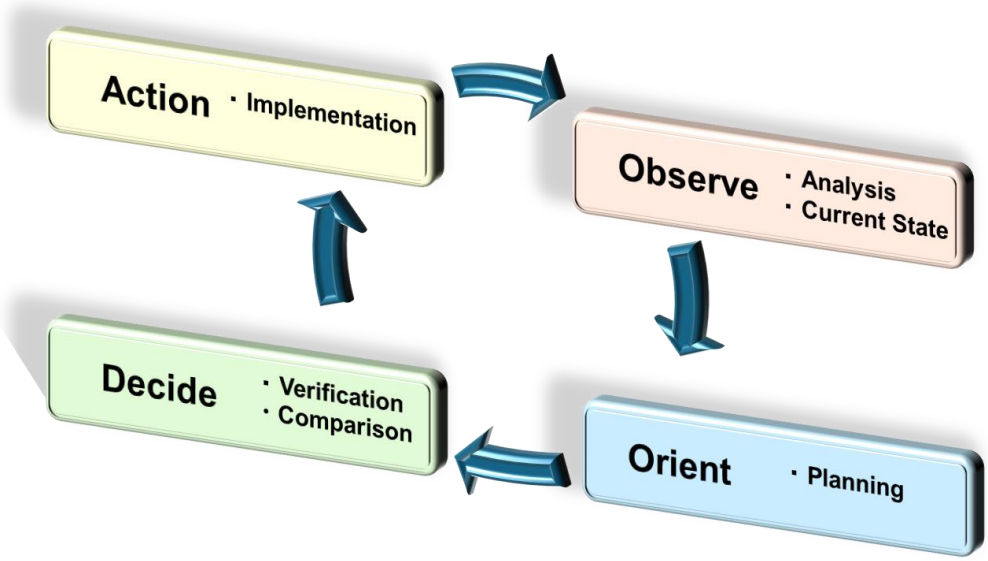

Figure 1. OODA Process Framework

The OODA loop comprises four major phases. A detailed description of each phase is provided below:

Phase: Observe (Observation)

Analysis: The latest IGVC 2026 official rulebook is analyzed to identify mission requirements and define the desired behavior and response of the mobile robot.

Current State: The team evaluates the performance limits and behavior of existing and past mobile robot designs, including the 2025 model, to understand current technical capabilities and challenges.

Phase: Orient

Planning: Based on the identified requirements and current capabilities, specific target values are established and core design policies are defined, including software and hardware system architecture, control strategies, and performance criteria required to achieve the desired behavior of the mobile robot.

Phase: Decide

Verification: Simulations and real-world outdoor experiments are conducted using the developed prototype mobile robot to collect empirical data for evaluation.

Comparison/Analysis: A quantitative comparison is performed between the measured data from these tests and the predefined target values.

Phase: Action

Implementation: Once it is confirmed that all requirements and desired behaviors of the mobile robot are satisfied, final system integration is carried out.

3.2 Definition of System and Subsystem Requirements

Based on the official IGVC 2026 rules, the evaluation of performance limits of prototype and past mobile robot designs, and operational knowledge from previous years, we defined 18 primary requirements (Table 1) to guide the design of the mobile robot. These requirements serve as evaluation criteria for verifying design validity throughout the development process. Detailed specifications for each requirement are provided in Chapters 4–9.

Table 1. Eighteen Primary Requirements

Category	Requirement	Measurement / Method	Target Value
Mechanical	Dimensions	Tape measure (exterior)	L 3.0 - 7.0 ft W 2.0 - 4.0 ft H - 6.0 ft
	Serviceability	Assembly Time	within 15 min
Safety	E-Stop distance	Braking distance (asphalt)	<1.0 ft (0.3m)
	Wireless E-Stop	Signal range test (outdoor)	100 ft <
Electrical	Runtime	Continuous operating time	2.0 h <
	Reliability	Inspect fuses/PSU/isolators	Operational Test Successful
Perception (AutoNav)	Lane detect	3D-LiDAR reflectivity data	≥16.4 ft (5.0 m)
	Obstacle detect	Detection test	1.6 – 30 ft (0.5 - 9.1 m)
Perception (SelfDrive)	Accuracy	AP on YOLOv8 test set	AP 0.85 or more
	Object distance	Camera detection limit	≥16.4 ft (5.0 m)
Driving Logic (AutoNav)	WP accuracy	GNSS vs. Estimated pos.	Error ≤ 2.5 ft
	Climbing ability	15% grade autonomous climb	No slip or stop
Driving Logic (SelfDrive)	Traffic rules	Log analysis at stop lines	Hold for 5.0 s
	Safety distance	Stopping distance from pedestrian	Stop at 5 – 7 ft
KPI (AutoNav)	Maximum speed	Measure speed	1.00 mph ≤
	Maneuver	5 ft narrow chicane test	90% Success
KPI (SelfDrive)	Latency	Object recognition speed	≤0.20 s
	Stop line	Deviation from target line	≤0.98 ft (30cm)

4 Mechanical Design

During the Observe and Orient phases of the OODA loop process, we analyzed the technical challenges identified during past mobile robot development, including the previous model (Orange2025), and established specific design requirements to address them. Table 2 and Figure 2 present a comparison of these requirements, along with a design comparison of the redesigned mobile robot.

Table 2. Mechanical design challenges and requirements

Problems	Requirements
Carrying problem to bring the moble robot from Japan to the U.S. It took time to assembly of moble robot.	Suitcase-sized Modularization with small In-wheel motors.
Casters at both ends caused In-wheel motors to lose ground contact on slopes.	Removal of front casters and payload relocation.

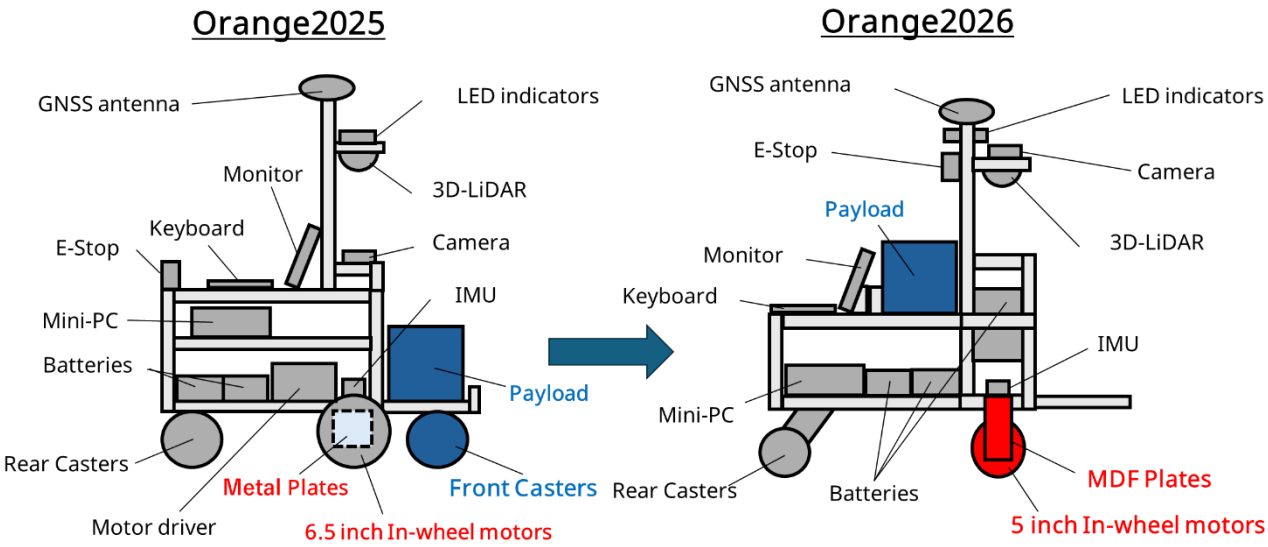

Figure 2. A design comparison of the overhauled mobile robot

4.1 Mobile Robot Chassis Modularization for Suitcase Storage

As illustrated in Figure 3, the mobile robot chassis and its associated components are modularized into three sections to fit within a suitcase that complies with the international carry-on baggage size requirements.

Module 1 Global Navigation Satellite System(GNSS) antenna, LED Indicator, camera

Module 2 In-wheel motors, motor driver

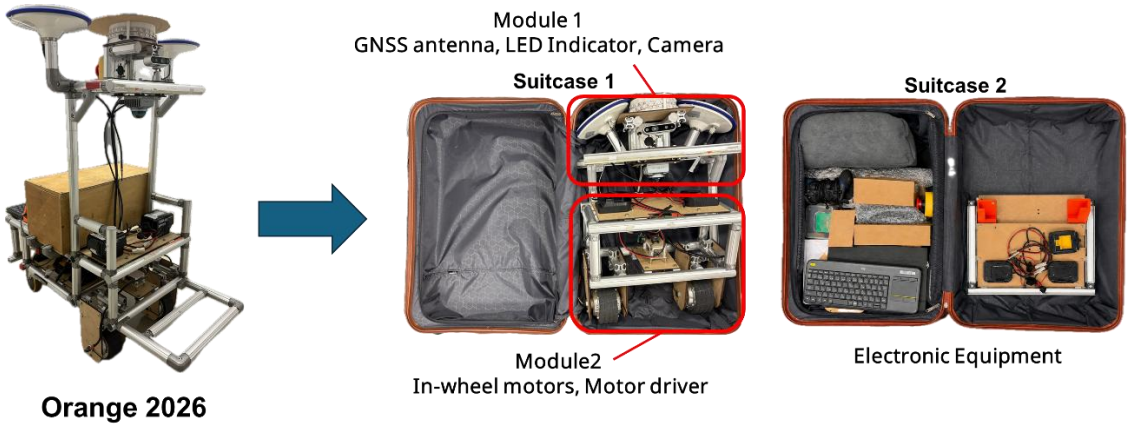

Figure 3. Storage status within a suitcase

4.2 Use of Smaller In-Wheel Motors

In last year's design, the large tire diameter (6.5 inches) posed a constraint for transportation, requiring tires and frames to be disassembled to fit into a suitcase. To address this issue, the new design adopts smaller tires (5-inch diameter), as shown in Figure 4, enabling the entire system to be transported in a single suitcase without module disassembly.

Figure 4. Size comparison of in-wheel

4.3 Modification of Tire and Frame Mounting Method

Due to the reduction in tire size, the conventional mounting method using custom metal plates is no longer suitable. In the previous design, the wheels were supported by a single axle and fixed using specially fabricated metal components. In the current design, the wheel support structure has been redesigned to provide support on both sides of the axle. The wheels are now fixed at both ends using medium-density fiberboard (MDF), which is sufficiently robust while being easily machinable within the laboratory. The previous metal components required outsourcing and took several weeks to manufacture, whereas the MDF components can be fabricated in a few hours. In addition, the use of MDF reduces the overall system weight, which is advantageous for transportation.

Figure 5. Mounting parts made from MDF

4.4 Enhancement of Ramp Climbing Ability

In last year's design, casters were installed at both the front and rear of the mobile robot to improve driving stability on flat terrain. Although this configuration enhanced stability during normal operation, it introduced a critical limitation during ramp traversal. As shown in Figure 6, when the mobile robot attempted to climb a steep slope, the drive wheels occasionally lost ground contact, resulting in a loss of traction and failure to ascend.

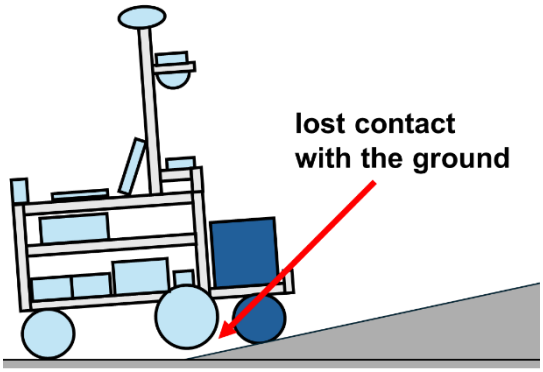

Figure 6. Traction loss of drive wheels on a ramp

To resolve this, the front caster was removed in the current design to improve climbing performance. In addition, the payload, which was previously located at the front, has been repositioned toward the center of the chassis to maintain driving stability and ensure sufficient ground contact of the drive wheels.

4.5 Evaluation of Mechanical Design Requirement Achievement

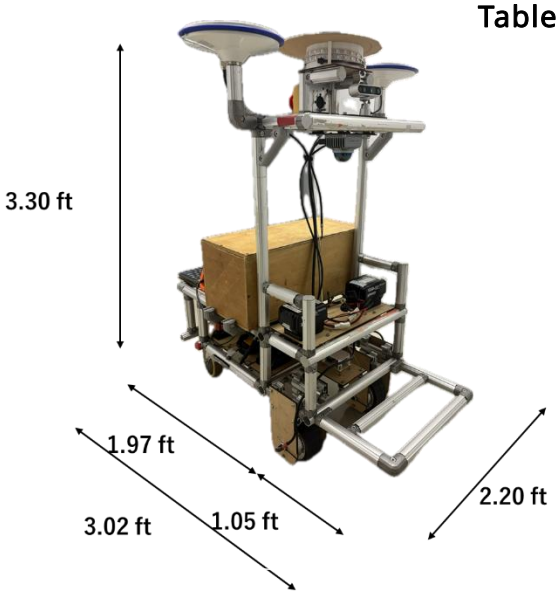

Figure 7. Orange2026

Table 3. Comparison of mechanical design requirements

Specification	Target value	Actual value
Length	3.0 - 7.0 ft	3.02 ft
Width	2.0 - 4.0 ft	2.20 ft
Height	- 6.0 ft	3.30 ft
Assembly time	Within 15 min	10 min 30 s

This section evaluates the specifications and dimensions of the developed mobile robot “Orange2026” (Figure 7).

The mobile robot’s dimensions fully comply with the official IGVC 2026 regulations. Because the chassis has been modularized into three separate modules to facilitate suitcase storage, both the reassembly time and packing efficiency have been considerably improved. As a result, the reassembly time is reduced to approximately 15 min.

5. Safety

5.1 Safety Measures for Operation

Table 4 summarizes the safety measures for the mobile robot during transportation, parking, and charging.

Table 4. Safety measures for operation

Operation Phase	Safety Measures
Transported	Disassemble the mobile robot into modules and physically remove the battery for suitcase storage.
Parked	Maintain active holding torque in the drive system while the mobile robot is stopped.
Charging	Charge the battery only after it has been completely removed from the mobile robot.

5.2 E-Stop System

To ensure safe operation, the mobile robot is equipped with both wired and wireless E-Stop systems that meet IGVC regulations.

Wired E-Stop: A 1-inch-diameter button is mounted on the rear of the chassis and directly connected to the motor driver. When pressed, it sends a stop signal directly to the motor driver, enabling an immediate halt without software intervention and thereby ensuring a fail-safe response.
Wireless E-Stop: A remote-controlled wireless E-Stop system has been developed to further enhance safety. A microcontroller (ESP32) receives signals from a handheld transmitter and transmits a stop command to the motor driver to halt the mobile robot.

5.3 Evaluation of Safety Requirements Achievement

Table 5 summarizes the safety requirements established in Chapter 3 and the results of their verification using the developed mobile robot.

Table 5: Comparison of E-Stop stopping distance and wireless E-Stop effective range

Requirement	Target value	Actual value
E-Stop stopping distance	< 1.0 ft	**0.8 ft**
Wireless E-Stop effective range	100 ft <	**125 ft**

The performance of the E-Stop system was evaluated by testing both wired and wireless functions while the mobile robot operated in autonomous navigation mode at a speed of 4 mph.

First, the wired E-Stop was evaluated by measuring the response time between button activation and system reaction, as well as the stopping distance. The stopping distance was determined by activating the E-Stop while the robot was traveling at 4 mph on an asphalt surface. The results showed an emergency stopping distance of 0.8 ft and

demonstrating superior braking performance.
Next, the wireless E-Stop was tested to verify its operational reliability. The results confirmed that reliable stop operations were achieved within a wireless communication range of up to 125 ft.

6. Electrical and Electronics Design

6.1 System Configuration and Key Components

Figure 8 illustrates the hardware layout and device placement of “Orange2026.”

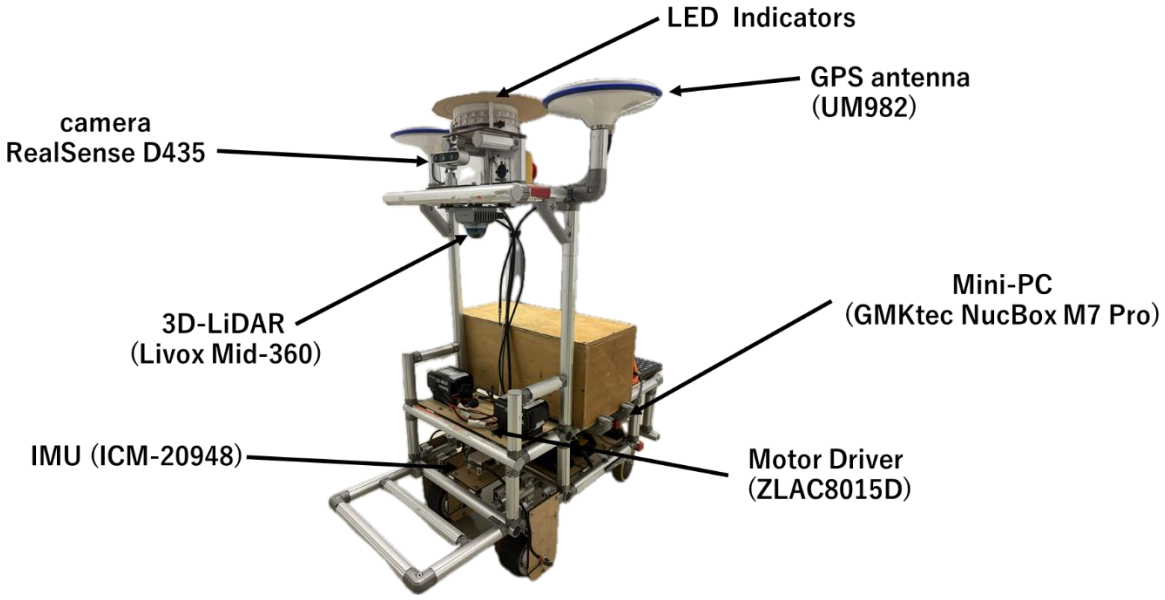

Figure 8. Device placement diagram

Mini PC (GMKtec NucBox M7 Pro): Equipped with an AMD Ryzen 9 PRO 6950H (8 cores/16 threads) and 32GB of DDR5 memory, this unit performs high-speed processing and integrates all sensor signals while managing the control commands for the motor drivers.
Motor Driver (ZLAC8015D): Controls the differential drive system and sends precise rotation commands to the in-wheel motors (ZLLG45ASM200).
3D LiDAR (Livox Mid-360): Captures the surrounding environment as high-density point cloud data. To enable real-time transmission of large data volumes, the sensor is connected to the Mini PC via Ethernet.
GNSS (UM982): Utilizes a dual-antenna configuration to obtain centimeter-level localization data and accurate heading (orientation) information.
IMU (ICM-20948): Measures the mobile robot’s attitude, angular velocity, and acceleration to support stable movement.
Camera (Intel RealSense D435): Captures front-facing RGB-D (color and depth) information, which is primarily used for semantic object recognition.
LED Indicators: Provide visual feedback on the current operational status of the mobile robot.

6.2 Power and Signal Design

Figure 9 illustrates the power and signal flow of “Orange2026.”

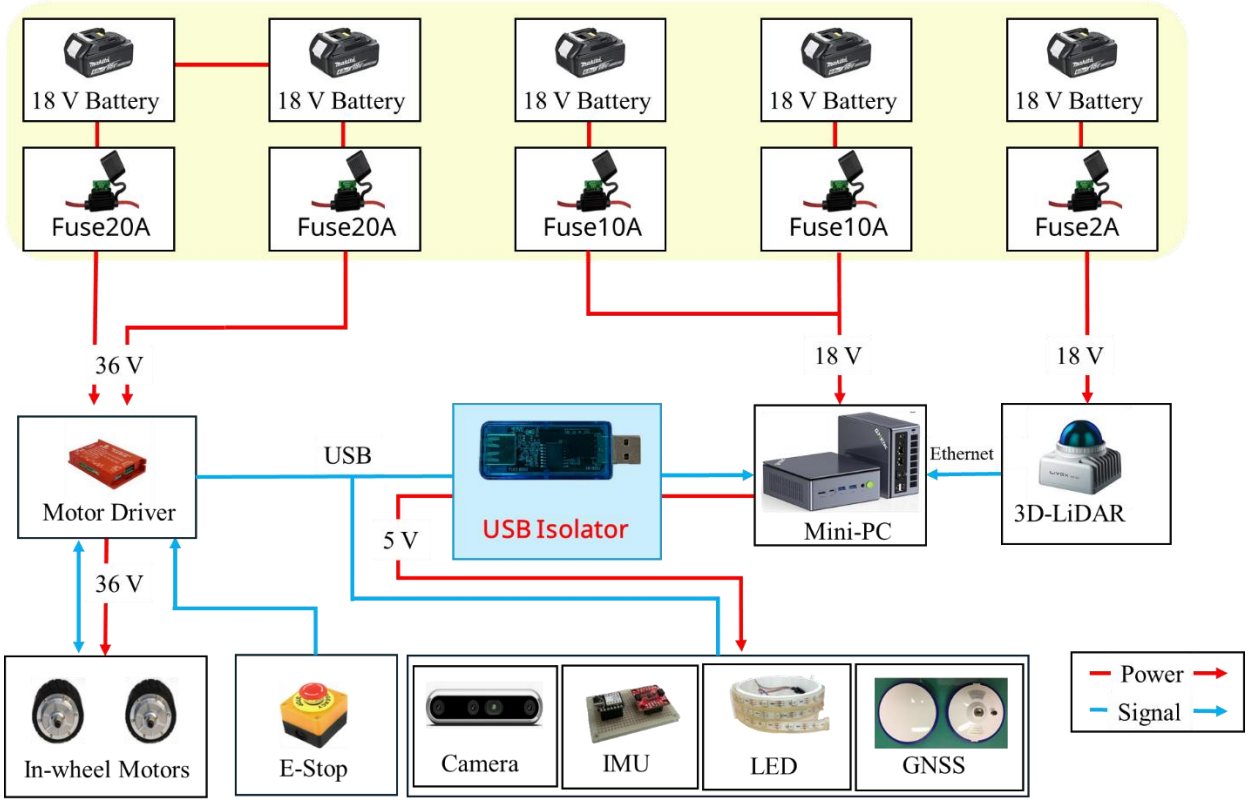

Figure 9. Power and signal flow

To enhance transportability and ensure a continuous power supply to the Mini PC, five small portable lithium-ion batteries are used. For safety, fuses are installed on all five batteries to prevent overcurrent damage to connected devices.

The power system is divided into separate lines for the motor drive and sensing/processing systems to reduce electrical interference and prevent unexpected interruptions to the Linux-based Mini PC.

The motor driver requires 36 V; therefore, two 18 V lithium-ion batteries are connected in series to meet this requirement. This configuration also helps reduce electrical noise that could affect other sensing devices.

For the Mini PC, two batteries are connected in parallel to provide a stable power supply. This configuration allows one battery to be replaced without shutting down the Mini PC, thereby ensuring continuous operation during experiments.

Furthermore, a USB power isolator is inserted between the Mini PC and connected USB devices to protect against surges and noise originating from USB-connected sensing devices or the motor driver.

Independent Power Supply System: To provide stable power to the PC, sensors, and motor drivers, the system adopts five independent battery cartridges.

Battery Selection: We utilized “Makita BL1860B (18 V, 6.0 Ah)” batteries for all power lines. Their built-in charge indicator markedly enhances operational efficiency and field usability.

Upgraded PC Power Supply: Compared with the last year’s model, in which the Mini PC was powered by a single battery, the current design employs two batteries in parallel.

This modification considerably extends the operational time of the mobile robot.
Installation of Fuses: Fuses are installed at the source of each power supply line to provide circuit protection by interrupting abnormal current flow during a short circuit.
Introduction of USB Isolators: A USB isolator is incorporated between the Mini PC and USB hub to provide electrical isolation, shielding the PC's circuitry from potential overvoltage or electrical leaks that may originate from motor drivers or external sensors.

6.3 Evaluation of Electrical Design Requirements Achievement

Table 6 presents the predefined electrical requirements and the corresponding verification results.

Table 6: Comparison of Electrical Design Requirements

Requirement	Target value	Actual value
Continuous operating time	2.0 hours <	**2.0 hours or more (Estimated value)**
Power supply seliability	Verification of Protection Circuit Operation	**Working properly**

Through experiments, we analyzed the Mini PC, which exhibited the highest power consumption in the mobile robot system. The verification tests demonstrated that the addition of two batteries in parallel to supply the Mini PC enables stable operation of the entire system for more than 2.0 h. Furthermore, the implementation and validation of protection circuits, including power supply fuses and USB isolators, result in a highly secure, noise-resistant electrical architecture.

7. Perception

7.1 Perception in AutoNav

Robust and stable recognition under varying weather conditions, such as strong sunlight and rain, is a key requirement for autonomous navigation (AutoNav). To address this, we focus on improving perception reliability.

To achieve weather- and illumination-independent perception, reflectivity information derived from 3D LiDAR point clouds is utilized.
Line Recognition: Figure 10 shows an image of line recognition using intensity (reflectivity) information obtained from the 3D LiDAR.

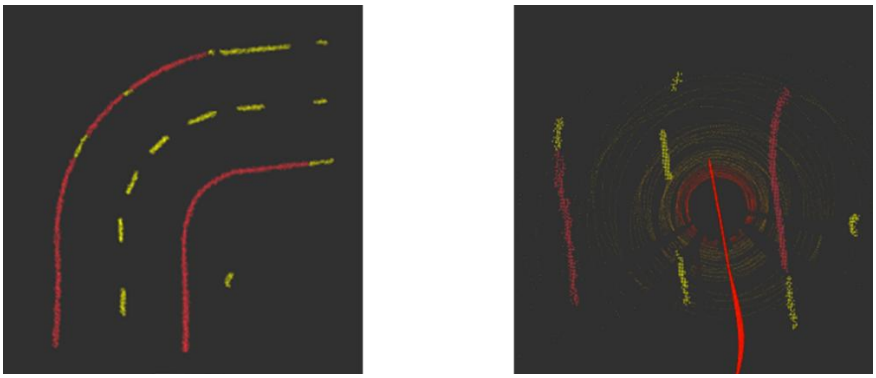

Figure 10. Line recognition using intensity information

First, the system applies intensity-based thresholding to the captured ground point cloud to extract high-reflectivity points as lane candidates. **Density-based**

spatial clustering of applications with noise is then applied to these extracted points to identify spatially continuous clusters as lines. Furthermore, the system classifies these clusters based on the number of points they contain: clusters with a large number of points are identified as solid lines, whereas those with fewer points are categorized as dashed lines. By directly processing the point cloud data, the proposed approach simplifies preprocessing, reduces computational load, and ensures stable line recognition.

Obstacle Avoidance: Ground Segmentation is performed to remove ground-level points from the LiDAR data. The remaining points are then clustered and identified as obstacles. This process enables real-time identification of barrels, barricades, and other randomly placed objects on the course, allowing for effective obstacle avoidance.

7.2 Perception in Self-Drive

In the Self-Drive Challenge, semantic recognition of objects and signs is essential. To address this requirement, we adopt an approach that combines a camera (Intel RealSense D435) with deep learning techniques.

Object Recognition and Text Identification via YOLOv8: As shown in Figure 11, object recognition is performed on camera images using YOLOv8.

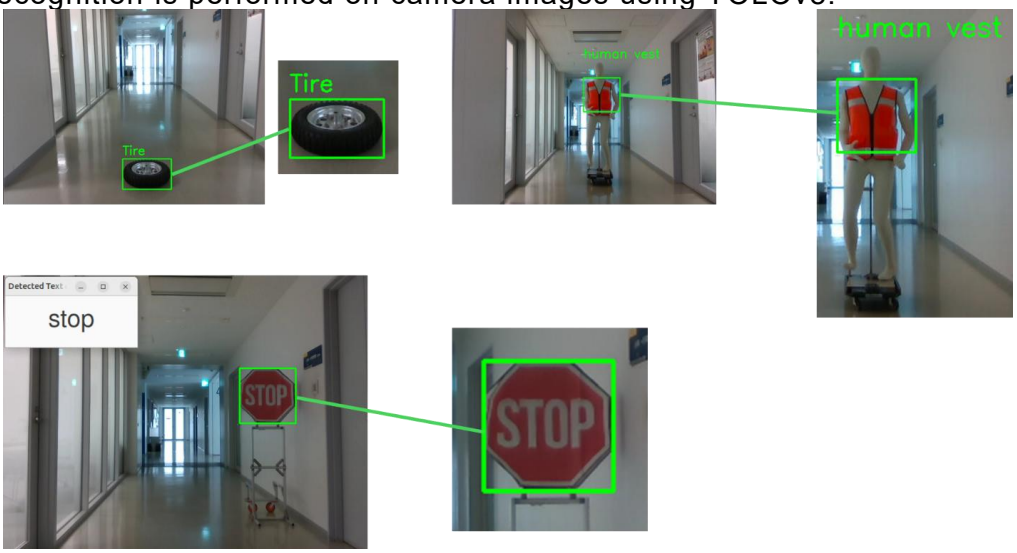

Figure 11. Object recognition results using YOLOv8 from camera images

We use **YOLOv8**, which has undergone transfer learning from a pre-trained model, to detect and classify STOP signs, pedestrians (mannequins), and tires in real time. Figure 12 illustrates the results of the sign text identification process.

Figure 12. Results of sign text identification

In addition to recognizing the STOP sign's shape and color, we implemented an algorithm to identify the text on the sign. This approach allows the system to reliably distinguish a true STOP sign from fake signs (such as those displaying "SOUP" or "IGVC"), which are expected under the competition rules.

7.3 Evaluation of Perception Requirements

To evaluate the performance of the designed perception system, the experimental results were compared with the predefined perception requirements (Table 7).

Table 7: Comparison of perception requirements

challenge	Requirement	Target value	Actual value
Auto Nav	White line detection distance	≥ 16.4 ft (5.0 m)	**21.7 ft (6.6 m)**
	Obstacle detection range	1.60 – 30.0 ft (0.5 - 9.1 m)	**1.97 – 42.7ft (0.6 -13m)**
Self Drive	Object recognition precision	AP 0.85 or more	**0.95**
	Object recognition distance	≥ 16.4 ft (5.0 m)	**18.0 ft (5.5 m)**

In line detection using 3D LiDAR reflectivity, stable detection was achieved up to 21.7 ft, exceeding the predefined target by 16.4 ft.

Additionally, obstacles within a range of 1.97–42.7 ft were detected using 3D LiDAR point clouds.

The minimum detection distance was measured at 1.97 ft, which is 0.37 ft greater than the initial target value of 1.6 ft. This difference is intentional, as a self-shape point cloud mask was applied to prevent the system from misidentifying the mobile robot's structure, such as its struts and frame, as obstacles.

Furthermore, in object identification using YOLOv8, a high recognition accuracy was achieved with an average precision of 0.95. An object recognition distance of 18.0 ft was also achieved, ensuring sufficient processing time for both safe braking at maximum speed and the identification of text on signs.

8. Driving Logic

8.1 Hierarchical Control Architecture

The navigation logic of “Orange2026” employs a hierarchical architecture operating on the ROS 2 framework. Figure 13 presents a block diagram of the system, illustrating the data flow from sensor acquisition to motor output.

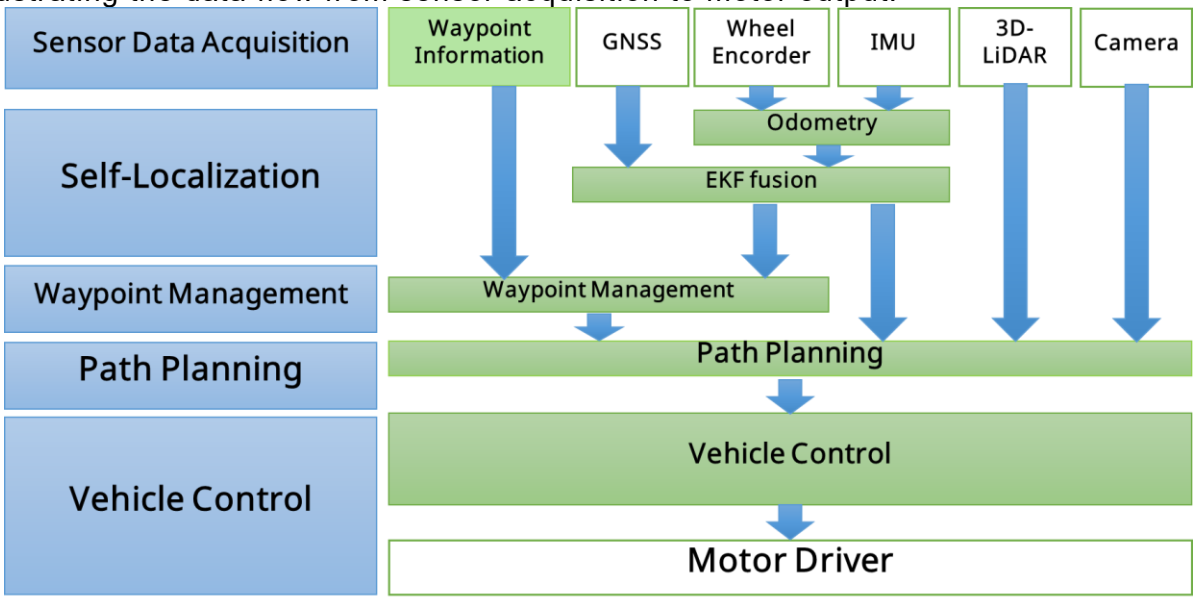

Figure 13. Software architecture block diagram

Sensor Data Acquisition: The system collects data from various sensors, including GNSS, wheel encoders, IMU, 3D LiDAR, and camera.

Self-Localization: Odometry is calculated by integrating encoder and IMU data. An extended Kalman filter (EKF) is then applied to fuse this odometry with GNSS information, enabling stable position estimation even in challenging outdoor environments.

Waypoint Management: The system manages and dynamically updates the next target destination by comparing pre-configured waypoint information with the current estimated position.

Path Planning: A navigation path is generated based on the target direction from the Waypoint Management module, the current position, and real-time obstacle information from 3D LiDAR and camera data.

Vehicle Control: Following the planned path, the system issues specific rotations per minute commands to the left and right wheel motors. Additionally, the control logic includes a state-switching mechanism that adjusts the driving mode based on perceived obstacle data.

8.2 Navigation in AutoNav

In the AutoNav Challenge, we deploy a driving strategy divided into eight segments, determined by the geometric characteristics of the course and the types of obstacles encountered. As shown in Figure 14, specific target objects for prioritized recognition are defined for each segment, and an optimal local path planning is selected accordingly.

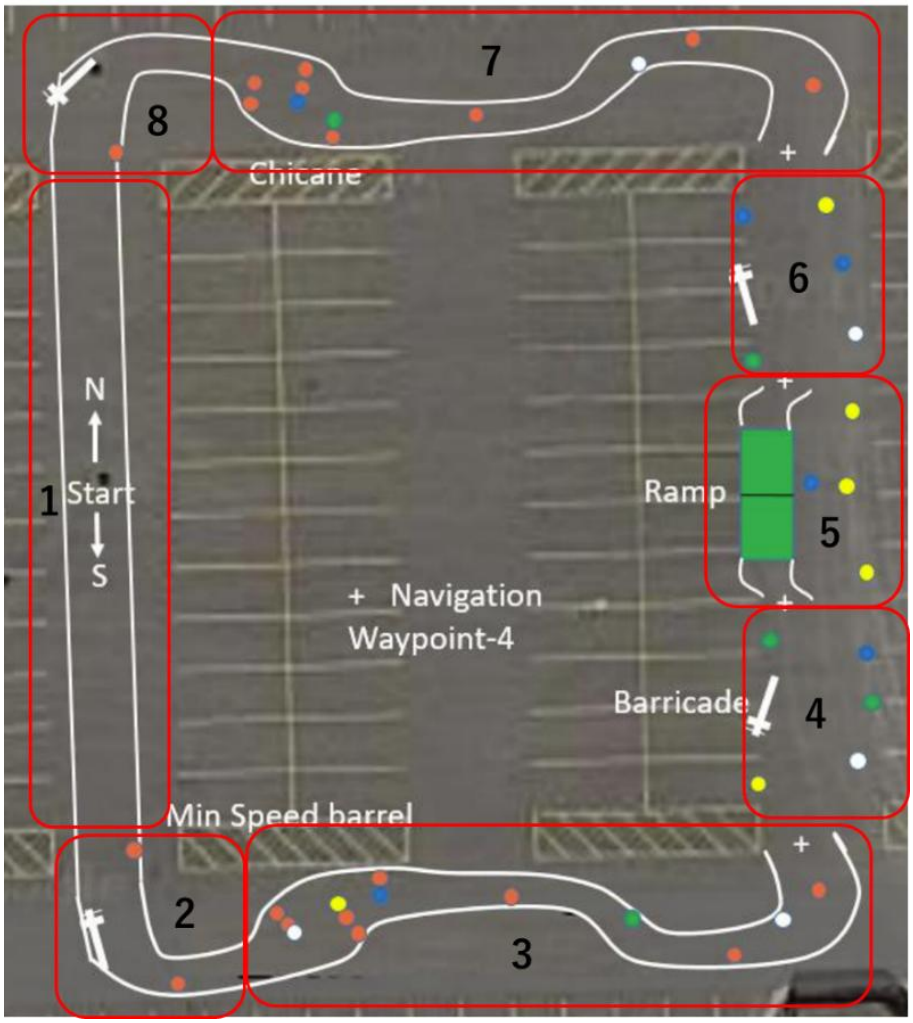

Figure 14. Segment division of the AutoNav course

Segment 1: The primary objective is lane keeping to ensure a stable cruising speed.

Segments 2, 3, 7, and 8: In these segments, the lane-bounded driving area is densely populated with obstacles, such as barrels and barricades. To navigate these, the system switches to reactive avoidance behavior based on the **potential field method** using LiDAR point cloud data.

Segments 4, 5, and 6: As lines are discontinuous in these segments, the system prioritizes self-localization using **GNSS (UM982)**. This enables accurate navigation without deviation from the driving area, even in the absence of physical boundary lines.

Segment 5 (Ramp): In the ramp area, the mobile robot detects the incline using LiDAR data and optimizes driving parameters to ensure sufficient torque for climbing the slope.

8.3 Driving Strategy in Self-Drive

In the Self-Drive Challenge, the mobile robot must complete 21 consecutive functions. Figure 15 illustrates these functions within the Self-Drive course and outlines the corresponding driving logic associated with each function.

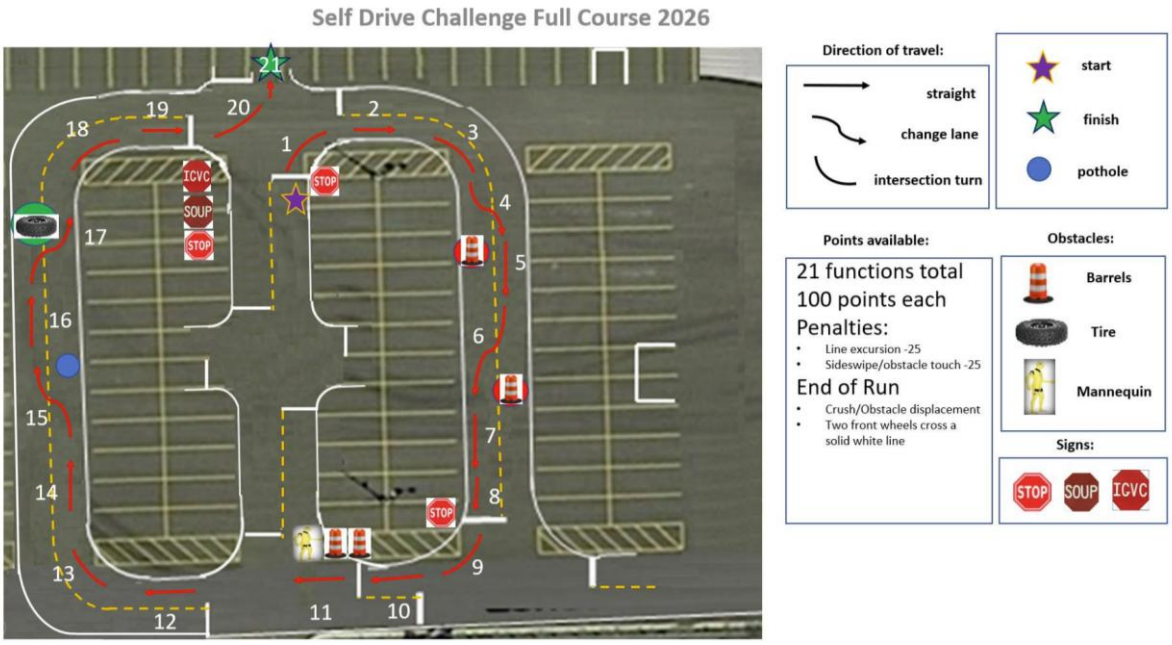

Figure 15. Twenty-One functions in the Self-Drive course

Lane Maintenance and Curved Paths (Functions 2, 3, 5, 8, 10, 12, 13, 14, 16, and 18): By identifying solid and dashed lines, the system prevents lane deviation while achieving smooth cornering performance.

Intersections and Sign Response (Functions 8 and 19): The system executes a complete 5-s stop, triggered by the recognition of STOP text via the camera and the detection of stop lines using LiDAR intensity data.

Static Obstacle Avoidance (Functions 4, 6, 15, and 17): Upon detecting barrels, potholes, or tires, the mobile robot selects a lane-change maneuver after ensuring the safety of the adjacent lane.

Dynamic Obstacle Avoidance (Function 11): When the system detects a mannequin (dynamic pedestrian) suddenly appearing from behind a barrel, it halts immediately while maintaining a prescribed safety distance of 5–7 ft. The control logic then enables automatic resumption of driving once the sensors confirm that the path is clear.

8.4 Evaluation of Driving Logic Requirement Achievement

Table 8 presents the driving logic requirements and corresponding verification results obtained from testing the actual mobile robot.

Table 8: Comparison of driving logic requirements

challenge	Requirement	Target value	Actual value
Auto Nav	WP arrival accuracy	Error ≤ 10.0 ft	8.2 ft
	Climbing ability	Completion of 15 % grade	Success
Self Drive	Stop-time duration	Hold for 5.0 s	5.1 s
	Pedestrian safety distance	Stop at 5 – 7 ft	5.5 ft

Verification experiments conducted on an outdoor test course showed that our

EKF-based position estimation utilizing the UM982 achieved a waypoint arrival accuracy of 8.2 ft. The waypoint acceptance radius was therefore set to 8.2 ft for autonomous navigation.

Furthermore, in the evaluation of climbing performance, the mobile robot successfully traversed a 15% gradient slope without stopping or exhibiting wheel slip. These results demonstrate that the system can navigate ramp sections without difficulty.

9. Key Performance Indicators (KPIs)

9.1 KPI for the AutoNav Challenge

For the AutoNav Challenge, two metrics were defined as KPIs in accordance with the competition rules. Table 9 summarizes the rationale for their selection, measurement methods, and target values.

Table 9: Defined key performance indicators (KPIs) for AutoNav

KPI	Rationale for selection	Measurement method	Target value
Minimum speed	To meet the minimum speed requirements for competition and ensure the course is completed within the time limit.	Calculate the minimum speed achieved during autonomous navigation on the test course.	**≥ 1.00 mph**
Mobility in narrow aisles	To evaluate the ability to navigate through the minimum path width (5 ft) and complex chicanes without contact.	Measure the success rate of non-contact runs on a test track with a width of 5.0 ft.	**90% Success Rate**

9.2 KPI for the Self-Drive Challenge

For the Self-Drive Challenge, two metrics were defined as KPIs. Table 10 presents the rationale for their selection, measurement methods, and target values.

Table 10: Key performance indicators (KPIs) for Self-Drive

KPI	Rationale for selection	Measurement method	Target value
Object recognition speed	To ensure real-time vehicle safety by responding to obstacles/signs without significant processing latency.	Measure the time from camera frame input to completion of classification and localization by **YOLOv8**.	**≤ 0.20 s**
Stopping accuracy	To prove the ability to stop precisely at designated positions (such as stop lines or obstacles) per the 30 cm regulation.	Measure the actual distance (deviation) between the vehicle's front bumper and the designated stop line.	**Within 30 cm (0.98 ft)**

9.3 Summarized Evaluation of KPIs

Performance verification was conducted for each system based on the defined KPIs. The results are summarized in Table 11.

Table 11: Comparison of target and key performance indicator values

challenge	Requirement	Target value	Actual value
Auto Nav	Minimum speed	1.00 mph ≤	1.12 mph
	Narrow space driving performance	90 % success rate	95 %
Self Drive	Object recognition speed	≤ 0.20 s	0.12 s
	Stopping accuracy	≤ 0.98 ft (30 cm)	0.39 ft (12 cm)

Analysis of the AutoNav Challenge:

The minimum speed of 1.12 mph satisfies the requirements stipulated in Rule I.2. Furthermore, a 95% success rate in narrow-passage navigation demonstrates the effectiveness of the proposed design, which limits the total mobile robot width to 2.2 ft, in combination with a high-precision LiDAR-based obstacle avoidance logic.

Analysis of the Self-Drive Challenge:

The object recognition speed (0.12 s) considerably exceeds the target value, ensuring a sufficient safety margin between obstacle detection and braking initiation during operation. The system also successfully meets the strict IGVC stopping accuracy criterion of “within 30 cm of the stop line,” demonstrating its high reliability.

10. Analysis of Complete Vehicle

10.1 Hardware Failure Points and Solutions

Table 12 summarizes the mechanical and electrical component issues identified during mobile robot testing, along with the corresponding solutions.

Table 12: Identified failures and countermeasures

Failure Points	Potential Causes	Countermeasures
Structural damage to MDF plate	Vibration and moisture absorption	Application of **waterproof coating** and using **double-layered MDF.**
Electrical short circuits	Complex wiring and contact failure from five independent power sources.	Install **fuses** on power lines and implement thorough cable management.
PC damage due to overvoltage	Abnormal voltage surges from connected USB devices.	Use **USB isolator** between the Mini-PC and USB hubs to protect internal circuits.

10.1.1 Structural damage to MDF plates

As shown in Figure 16, replacing metal plates with MDF introduced issues related to operational vibrations, moisture absorption, and deformation of the MDF, causing the wheel axle to lose horizontal alignment. To address this, a waterproof spray coating was applied, and a two-layer structure using 2.5 mm-thick MDF was adopted for the chassis design. Furthermore, considering the mechanical strength of MDF, the wheel support structure was changed from a single-sided to a double-sided axle configuration, providing support from both sides. Verification results showed no damage after several months of outdoor field testing, demonstrating sufficient durability for practical operation.

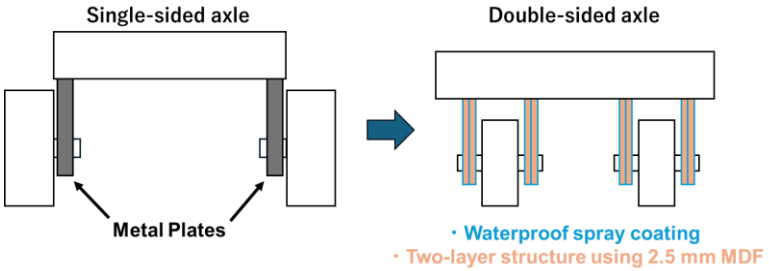

Figure 16. Comparison of Axle Structures

10.1.2 Electrical Short Circuits and PC Damage from Overvoltage

The adoption of an independent power supply system led to instances of short circuits caused by wiring issues. To address this, fuses were installed at the source of the battery wiring, establishing a protection circuit that physically interrupts abnormal current flow.

Furthermore, to protect the Mini PC from overvoltage spikes originating from connected devices, a USB isolator was integrated into the system, shielding the main PC from potential damage, even during unforeseen electrical failure.

10.2 Course Reproduction and Verification using Gazebo

A virtual digital twin environment was developed in Gazebo to simulate the Self-Drive Challenge (Figure 17).

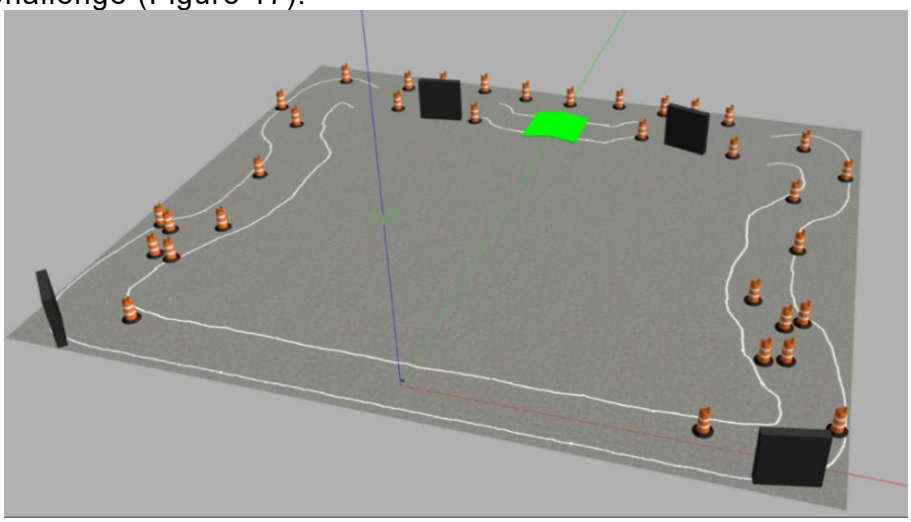

Figure 17. Virtual environment created in Gazebo

This environment incorporates lines, obstacles, and ramps, replicating actual competition conditions. By utilizing this simulation environment before real-world testing, we were able to safely and efficiently validate the performance of the newly developed software programs.

11. Cyber Security

Using the risk management framework and an analysis of recent vulnerabilities reported in the national vulnerability database (NVD), we identified three critical areas requiring particular attention in the developed mobile robot: container-related issues, Bluetooth communication vulnerabilities, and ROS 2 navigation system risks. Recent NVD reports indicate that Bluetooth vulnerabilities can cause system crashes or weakened encryption, while ROS 2 navigation components may expose the system to arbitrary code execution or remote attacks. These findings highlight that vulnerabilities across these three areas have become increasingly prominent. The following sections describe each risk and the corresponding countermeasures implemented with a view toward future mass production.

11.1 Insufficient Container Isolation and Execution Environment Vulnerabilities

These include a credential validation bypass in Moby (the foundation of Docker) (CVE-2026-33997) and server-side request forgery in AI model execution environments (CVE-2026-33990).

Countermeasures:

To mitigate these risks, the system enforces timely updates to the latest Docker Engine version and introduce image scanning based on a software bill of materials. In addition, the network configuration has been redesigned based on the principle of least privilege, and the use of privileged containers is prohibited to prevent potential intrusions at the execution environment layer.

11.2 Accumulation of Bluetooth Vulnerabilities and Authentication/Denial-of-Service (DoS) Risks

According to the NVD, as of April 2026, the number of Bluetooth-related vulnerabilities has reached 1,081. Notable examples include authentication bypass via capture-replay attacks (CVE-2026-4583) and DoS attacks through malicious frame transmission (CVE-2026-31280). These vulnerabilities pose direct risks, such as disabling of the wireless E-Stop or unauthorized operation of the mobile robot.

Countermeasures:

The wireless communication path is designed as a safety-related part of the control system) in accordance with ISO 13849-1 Performance Level d. For binary (ON/OFF) signal transmission, communication authenticity is prioritized over confidentiality. Message authentication is implemented using sequence numbering and expected-value verification, effectively mitigating systematic failures, such as replay attacks and command injection. This architecture ensures high diagnostic coverage for safety functions.

11.3 Vulnerabilities in ROS 2 Navigation2

A vulnerability in the nav2_mppi_controller of ROS 2 Navigation2 (Nav2) (CVE-2024-41647) may allow arbitrary code execution owing to improper permission settings, potentially enabling an attacker to gain full control over the mobile robot’s motion.

Countermeasures:

The system is kept updated to the latest software version containing relevant security patches. Furthermore, administrative and execution roles are separated, and appropriate permissions are assigned to each process based on the principle of least privilege. These measures considerably minimize the risk of unauthorized access or code execution.